 doi:10.20944/preprints202210.0123.v1

Article

Advanced Analysis of Electroretinograms Based on Wavelet Scalogram Processing

Aleksei Zhdanov [1]*, Anton Dolganov [1], Dario Zanca [2], Vasilii Borisov [1], and Mikhail Ronkin [1]

[1] School of Information Technologies, Telecommunications and Control Systems, Ural Federal University named after the first President of Russia B. N. Yeltsin, Yekatrinburg, Russia
[2] Machine Learning and Data Analytics Lab, Department Artificial Intelligence in Biomedical Engineering (AIBE), Friedrich-Alexander-Universität Erlangen-Nürnberg (FAU), Erlangen, Germany

Featured Application: The results of this work will be applied to the development of a system to assist ophthalmologist doctor decisions

Abstract: The electroretinography (ERG) is a diagnostic test that measures the electrical activity of the retina in response to a light stimulus. This test has a long history and has been extensively studied among years. Dr. James Dewar recorded the first electroretinogram signal in 1873. Later he described signal analysis using 4 components, namely amplitude, and latency of a-wave and b-wave. Nowadays, the international electrophysiology community has established the standard for electroretinography in 2008. However, from the point of view of signal analysis, the major change did not happen. ERG analysis is still based on the 4 components evaluation. The article describes ERG database including the classification of signals by using advanced analysis of electroretinograms based on wavelet scalogram processing. To implement an extended analysis of the ERG, the parameters extracted from the wavelet scalogram of the signal were obtained using digital image processing and machine learning methods. The results of the study show that the proposed algorithm implements the classification of adult electroretinogram signals by 19% more accurately and pediatric signals by 20% more accurately than the classical algorithm. The promising use of ERG is differential diagnostics, which may also be used in preclinical toxicology and experimental modeling. The problem of developing methods for electrophysiological signals analysis in ophthalmology is associated with the complex morphological structure of electrophysiological signals components, due to the generation of retina cell electrical responses to light stimulus.

Keywords: biomedical research; classification; machine learning; electroretinography; electroretinogram; ERG

1. Introduction

Biomedical research is multidisciplinary area of medicine, biology, informatics and engineering. The results of research in this area allows to develop new methods of diagnostics and treatment of various diseases [1]. The present study describes the use of biomedical ophthalmic signals for the diagnosis of retinal diseases.

To evaluate the retinal function by measuring electrical responses of the retina cells generated by light stimulus, the non-invasive ocular test calls electroretinogram (ERG) are using. ERG consists of several responses, namely, the photoreceptors in the outer retina, inner retinal layers, and the final output neurons [2]. ERG most used for diagnostic assessment of toxic retinopathies, diabetic retinopathies, hereditary diseases, etc.

Phenomenon of having electrical potential of living entities eye under light stimulus action was founded physician Holmgren originally Swedish in 1865. This was the background for scientific discovery of ERG. Further studies of Dewar, Einthroven, Waller, and Granit identified ERG signals components conditioned by physiological responses [3–6] .

 doi:10.20944/preprints202210.0123.v1

Modern concept of ERG analysis involves measurement of a- and b-wave. a-wave is characterized as the first large negative component associated with photoreceptors response in the outer retina. b-wave describes positive component associated with inner layers response of the retina [7–11].

ERG technique has a great potential in the ophtalmology field for early disease detection, diagnosis, and intervention. Among this technique also, optical coherence tomography (OCT) test is mainly used. The ERG can be a useful addition for the patients who are children, cognitively or physically disabled, or in some other way cannot participate. In addition, it can reflect the retinal lesion several years before the visual symptomatology or structural damage detected by OCT. In the last recent years, ocular toxicity method has an increased popularity for drug therapy assessment on the visual impairment, where ERG technique has shown a good prospect in the retinal toxicity test [12,13]. However, manual ERG analysis greatly depends on the experience of the clinicians, the misdiagnosis will make the patients miss the best time or therapy for treatment. Automated algorithm will be a powerful tool for ERG signal analysis, but it requires large databases for verification and validation. The strong motivation to understand in more detail the ERG signals start in a first glance with building a signal's database which includes adult and children. In this way, waveforms can be analyzed from physiological process point of views and compared in terms of waveform morphology.

2. Related Work

The ERG signal is a complex signal which shows the electrical activity of retinal cells after stimulation. It should be noted that the ERG is a short duration signal which contains many spectral components. ERG is high frequency (2 kHz) and short (200 ms), therefore, the signal spectrum is in the range from 0 to 1 kHz, the spectrum sampling is 7.5 Hz, the useful information is distributed non-linearly and may appear in a narrower range. Currently, the ERG is evaluated using the amplitude and latency of the known waves in this signal.

The current scientific literature presents studies on the analysis of ERG in the frequency domain mainly based on the Fast Fourier transform (FFT), power spectral density (PSD), and linear prediction (LP) [14]. Scientific articles show a variety of research methods in the field of diagnosing diseases of the retina, but the results are difficult to generalize due to differences in ERG protocols. The methods presented in the articles demonstrate the accuracy of the analysis at the analysis level in the time domain. Some research is focused on the frequency domain analysis of the oscillatory potential. Since this signal has a shorter amplitude than other ERG components.

Obviously, the disadvantage of the FFT method is the lack of temporal localization, which means that the power spectrum density cannot provide information about the specific frequencies of the signal. To solve this problem, Short-time Fourier transform (STFT) was proposed to analyze small sections of the signal using a window [15]. Thus, STFT served as the basis for time-frequency analysis.

It is known from studies that a smaller window size leads to improved temporal resolution and reduces the number of discrete frequencies components. Thus, the wavelet analysis provides the full analysis potential for discriminate the ERG components.

The use of wavelet analysis (WA) has some advantages over other frequency-domain methods. It has a different window size, better suited for analyzing sudden and short-term signal changes. Most of the articles on ERG analysis in the time-frequency domain describe the use of continuous wavelet transform (CWT) and discrete wavelet transform (DWT) [16]. The first wavelet type requires more computation, resulting in a slower processing time compared to the discrete one. When using DWT, it is possible to lose some information if the correct level of decomposition is not chosen. When analyzing WA, two important factors should be considered the wavelet type and decomposition. Other papers which describe time-frequency domain analysis are also based on DWT technique. Both CWT and DWT methods have their specific advantages and disadvantages. CWT is more reliable than

 doi:10.20944/preprints202210.0123.v1

DWT because it can extract all available information without down sampling. However, CWT requires more computation, resulting in a slower process compared to DWT [17].

Moreover, CWT has property to be highly redundant, which is beneficial from one point of view and a curse from another. Because of it, no information is lost, unlike DWT. In DWT, it is possible to lose some useful information if the correct level of decomposition is not chosen. When analyzing WA, two important factors should be considered: the wavelet type and decomposition.

The above methods have the potential to extract needed information from the ERG signals where the feature extraction method and reference database must be carefully evaluated.

3. Material and methods

The study used a database of electroretinogram signals, which includes five protocols of adult and pediatric electroretinogram signals [18]: Scotopic 2.0 ERG Response (53 pediatric signals, 23 adult signals), Maximum 2.0 ERG Response (80 pediatric signals, 42 adult signals) , Photopic 2.0 ERG Response (74 pediatric signals, 32 adult signals), Photopic 2.0 EGR Flicker Response (63 pediatric signals, 38 adult signals), and Scotopic 2.0 ERG Oscillatory Potentials (20 signals). Electrophysiological studies were conducted at the IRTC Eye Microsurgery Ekaterinburg Center. Registration of electroretinogram signals was performed using a computerized electrophysiological workstation EP-1000, manufactured by Tomey GmbH.

The current analysis of the ERG signal is based on the assessment of the amplitude a, b and the latency l_a, l_b of the a- and b-waves (Fig. 1a). In addition to the analysis of the current parameters of the ERG signal, it is proposed to extract the parameters from the wavelet scalogram (Fig. 1b). To obtain the coupled components of the ERG signal, it is necessary to perform the following processing of the wavelet scalogram:

- Converting the scalogram values into 8-bit encoding format (value range from 0 to 255).
- Image binarization using the Otsu method.
- Image erosion with a 3 by 3-pixel kernel to remove local artifacts associated with digital signal processing. Erosion of the image allows you to remove pixels at the boundaries of the segments.
- Determine the connected components of the wavelet scale using the connected Components function from the OpenCV library.

The mathematical meaning of the connected components is a set of numbers Markers, which has the size of an image and carries information about the belonging of each point of the wavelet scale chart to a particular segment.

Table 1 describes the parameters extracted from the wavelet scalogram of ERG, divided into segments from 1 to 6 (Fig. 1b).

4. Statistical analysis of electroretinogram signal database

Prior to machine learning application the data was analyzed. The following measures were considered to ensure consistent results: it was ensured that each wavelet scalogram has all 4 segments correctly identified. If some of the segments was missing that such signal was not considered in final analysis. Most of such cases were for subjects with pathology. However, it is worthy of further detailed analysis whether having all segments to be presented on wavelet scalogram and correctly identified as a feature for express diagnosis. This analysis is out of scope for this paper.

4.1. Pediatric Group

For a pediatric group 65 signals were used for the analysis. Among them 26 we diagnosed as healthy and 39 as subjects with pathology. Table 2 presents the obtained amplitude and latency values for the a-waves and b-waves. According to the ISCEV Standard the result's table contained median values, standard deviation (STD), 5-th and

Preprints (www.preprints.org) | NOT PEER-REVIEWED | Posted: 10 October 2022 doi:10.20944/preprints202210.0123.v1

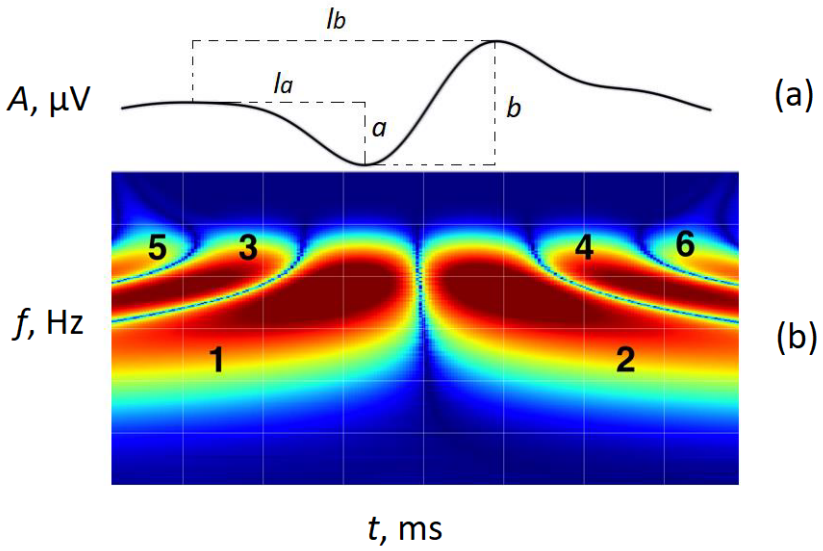

Figure 1. Amplitude-time (a) and frequency-time (b) representation of the electroretinogram signal.

Table 1. Parameters of electroretinogram signal.

Designation	Name	Description
B_{max}	maximum brightness of the wavelet scalogram segment	estimation of the segment amplitude in the selected frequency and time domains over the entire area (Fig. 2a)
f, t	frequency and time of the maximum region of the wavelet scalogram segment	estimation of the frequency-time coordinates of the maximum area of the analyzed segment associated with the prevalence of the specific cells or cellular structures contribution (Fig. 2b)
A_{median}	median brightness values from of wavelet scalogram segment	evaluation of the brightness distribution over the entire area of the analyzed segment (Fig. 2c)
A_{mean}	mean brightness values from of wavelet scalogram segment	assessment of segment displacement and uniformity of brightness distribution over the entire area of the analyzed segment (Fig. 2c)
t_1, t_2, f_1, f_2	frequency and time extremes of the wavelet scalogram segment	evaluation of the spatial location of the analyzed segment on the wavelet scalogram, (Fig. 2d)
$t_{1_{90}}, t_{2_{90}}, f_{1_{90}}, f_{2_{90}}$	frequency and time extremes of the wavelet scalogram 90% segment	evaluation of the spatial location of the analyzed segment, where amplitude is higher than 90% of maximum value

Preprints (www.preprints.org) | NOT PEER-REVIEWED | Posted: 10 October 2022 doi:10.20944/preprints202210.0123.v1

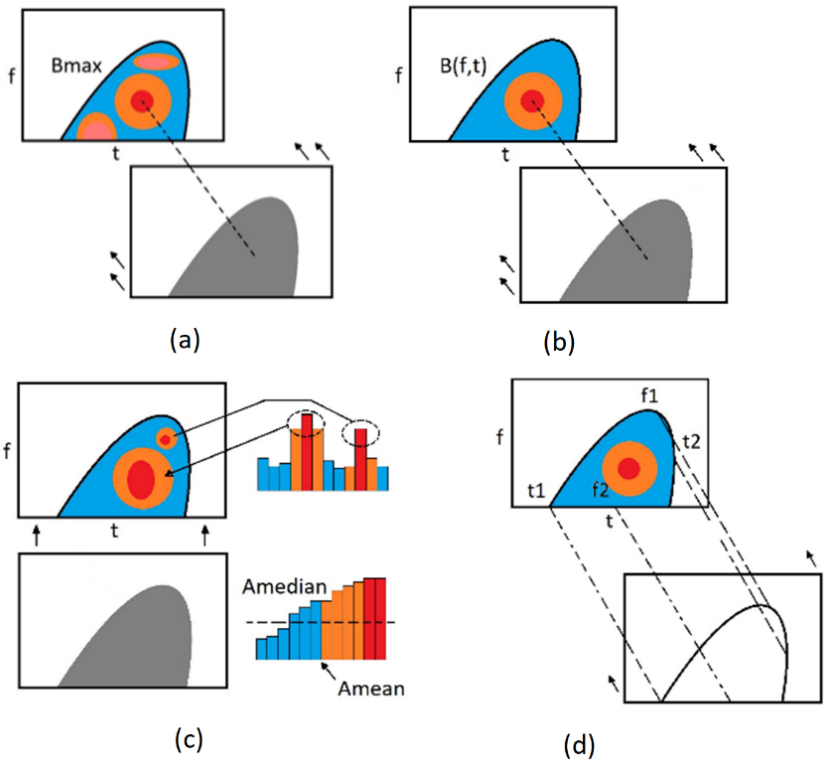

Figure 2. Parameters extracted from the wavelet scalogram of electroretinogram signal: (a) maximum brightness of the wavelet scalogram segment; (b) frequency and time of the maximum region of the wavelet scalogram segment; (c) median and mean brightness values from of wavelet scalogram segment; (d) frequency and time extremes of the wavelet scalogram segment

95-th quantile (Q5% and Q95%). The data is aggregated by the diagnosis. In the Fig. 3a are plotted the boxplots of amplitude and latency values for the a-waves and b-waves.

From data written in Table 2 and Fig. 3a one can conclude the following: the amplitude values seem to be better indicators to distinguish between two diagnosis groups. The subjects with pathology tend to have lower values of amplitude. However, it is worthy to mention that there are "overlaps" which makes improbable diagnostic using a single feature.

4.2. Adults Group

For an adults' group 38 signals were used for the analysis. Among them 11 we diagnosed as healthy and 27 as subjects with pathology. Table 2 presents the values of amplitudes and latencies for A and B waves. According to the ISCEV Standard we present median values, standard deviation (STD), 5-th and 95-th quantile (Q5% and Q95%). The data is aggregated by the diagnosis. Fig. 3b demonstrates the boxplots of amplitudes and latencies for *a*- and *b*-waves.

From data presented in Table 2 and Fig. 3b one can conclude the following: only the *b*-wave amplitude seems to work as an indicator to distinguish between two diagnosis groups. The subjects with pathology tend to have lower values of amplitude. Also, one can mention the latency of *a*-wave, as the subjects with pathology tend to have higher values. However again, it is worthy to mention that there are "overlaps" which makes improbable diagnostic using a single feature.

5. Results

The machine learning A machine learning approach was used to predict the diagnosis of the subjects (healthy or person with pathology) using features of biomedical signals.

Preprints (www.preprints.org) | NOT PEER-REVIEWED | Posted: 10 October 2022 doi:10.20944/preprints202210.0123.v1

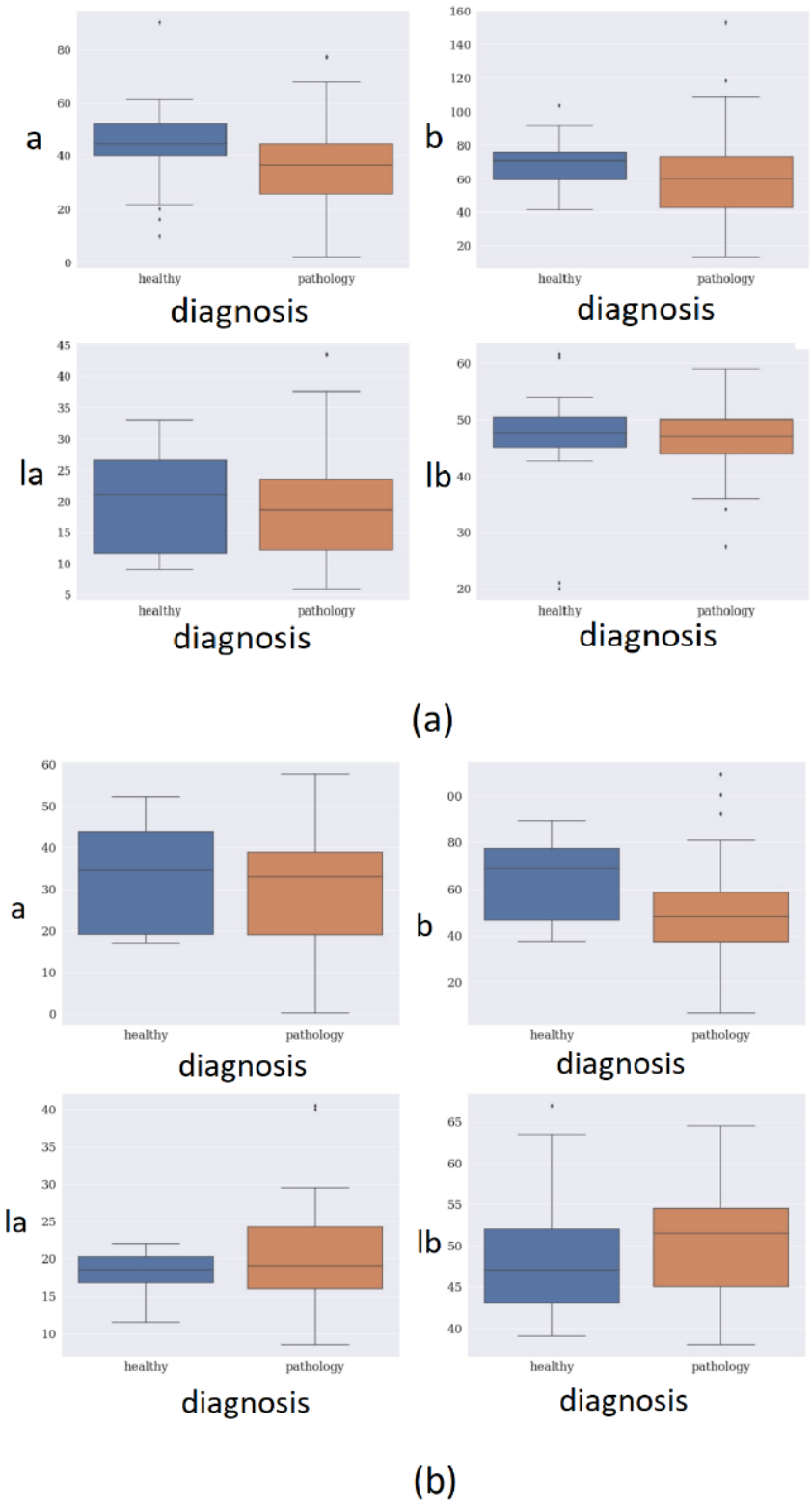

Figure 3. Boxplots of amplitudes and latencies for *a*- and *b*-waves: (a) pediatric group; (b) adults' group

Preprints (www.preprints.org) | NOT PEER-REVIEWED | Posted: 10 October 2022 doi:10.20944/preprints202210.0123.v1

Table 2. Values of amplitudes and latencies for a- and b-waves for pediatric and adults' group.

Group	Diagnosis	Median	STD	Q5%	Q95%
		a			
Pediatric	healthy	44.42	16.06	17.10	60.51
	pathology	36.47	17.06	6.46	59.83
Adults	healthy	34.51	13.30	17.53	50.38
	pathology	32.99	15.33	5.19	54.39
		b			
Pediatric	healthy	70.37	13.97	47.81	89.03
	pathology	60.13	27.91	18.94	109.57
Adults	healthy	68.73	19.47	37.52	88.52
	pathology	48.44	24.22	17.70	97.95
		l_a			
Pediatric	healthy	21.00	7.71	9.38	32.38
	pathology	18.50	8.32	8.35	33.00
Adults	healthy	18.50	3.41	12.25	21.75
	pathology	19.00	7.89	10.50	36.85
		l_b			
Pediatric	healthy	47.50	9.02	26.38	59.25
	pathology	47.00	7.01	35.80	59.00
Adults	healthy	47.00	9.16	39.25	65.25
	pathology	51.50	7.20	39.15	62.20

It was relevant for us to identify the usefulness of the new wavelet scalogram features. Because of that different groups of signals were considered separately:

- current features (amplitude a, b and the latency l_a, l_b of the a- and b-waves) (CF);
- wavelet analysis features for the 1 and 2 segments (WA1-2);
- wavelet analysis features for the 1, 2, 3 and 4 segments (WA1-4);
- joined list of current features and wavelet analysis features for the 1- 4 segments (CF+WA1-4).

The decision trees (DT) were selected as a machine learning method. The main reasoning to choose DT is an ability to select the most significant features for the task.

As DT tend to easily overfit the data it is of great importance to carefully tune the hyperparameters. For this study, the tuning of the following hyperparameters were considered *max_depth* (in range 1,2,...14,15) and *min_samples_split* (in range 3,6,...,12,15).

For each of 4 different groups of signals the most optimal hyperparameters were found using the GridSearch grid search using a 5-fold StratifiedKFold stratified K-fold cross-validation. After finding optimal hyperparameters the training and evaluating of model was as follows. First, we fit DT with the whole data. Then we select significant features using the feature_importances attribute only features with non-zero values of feature_importances were selected for subsequent analysis. Afterwards, we perform cross-validation of the DT model using only important features. The cross-validation was performed using StratifiedKFold implementation to ensure that each fold preserves the percentage of samples for each class. Number of splits was set to 5. The standard classification metrics were used – Accuracy, Precision, Recall and F1-score. To get the final evaluation of the DT model we have averaged metrics over all 5 validation folds. The standard deviation of the metrics over 5 validation folds was also considered. Table 3 presents values of the classification metrics for the pediatric group.

It is worthy to mention mentioning that with the above-described approach of fitting DT on whole data to select significant features and performing cross-validation check afterwards might introduce data leakage. However, given the limited amount of data at hand, it was not feasible to evaluate features importance on a subset of train data.

Preprints (www.preprints.org) | NOT PEER-REVIEWED | Posted: 10 October 2022 doi:10.20944/preprints202210.0123.v1

Table 3. Values of amplitudes and latencies for *a*- and *b*-waves for pediatric and adults' group.

Features Set	Metric	Accuracy	F1	Precision	Recall
Pediatric CF	Mean	0.52	0.52	0.72	0.52
	STD	0.06	0.18	0.19	0.32
Adults CF	Mean	0.54	0.62	0.55	0.73
	STD	0.24	0.35	0.31	0.43
Pediatric WA1-4	Mean	**0.70**	**0.74**	**0.78**	**0.76**
	STD	0.18	0.15	0.17	0.24
Adults WA1-4	Mean	0.78	0.84	0.86	0.84
	STD	0.23	0.17	0.19	0.16
Pediatric WA1-4	Mean	0.60	0.64	0.70	0.61
	STD	0.06	0.05	0.08	0.12
Adults WA1-4	Mean	0.81	0.86	0.87	**0.88**
	STD	0.20	0.14	0.17	0.17
Pediatric CF+WA1-4	Mean	0.58	0.65	0.66	0.66
	STD	0.10	0.07	0.07	0.10
Adults CF+WA1-4	Mean	**0.83**	**0.88**	**0.89**	**0.88**
	STD	0.10	0.07	0.07	0.10

5.1. Pediatric Group

For CF features set the following features were considered important: b.

For WA1-2 features set the following features were considered important (the number denotes the segment number of the wavelet scalogram): $B_{max}1$, $A_{median}1$, $t_1 2$, $f_{1_{90}}1$.

For WA1-4 features set the following features were considered important: $A_{median}1$, $A_{mean}1$, $A_{median}3$, $A_{mean}3$, $f_1 3$, $t4$, $t_2 4$, $t_{2_{90}}4$.

For CF+WA1-4 features set the following features were considered important: l_a, $A_{median}3$, $A_{mean}3$, $t4$.

Judging from data in Table 3 we can conclude that proposed new WA features seems to provide more robust and consistent models, compared to using Classical features.

Analyzing lists of important features one can draw the following conclusion: the WA features of the segment 1 and 2 seems to have the higher classification "power" than WA features if segment 3 and 4. At the same time the Classical Features seems to better complement WA features of the segment 3 and 4.

Table 3 shows values of the classification metrics for the adults group.

5.2. Adults Group

For CF features set the following features were considered important: a, b, l_b.

For WA1-2 features set the following features were considered important: $t_{1_{90}}1$, $t2$.

For WA1-4 features set the following features were considered important: $t_{1_{90}}1$, $t_{2_{90}}2$.

For CF+WA1-4 features set the following features were considered important: l_b, $t1$, $t_{1_{90}}1$, $t2$, $A_{median}2$.

Judging from data in Table 3 we can conclude that proposed new WA features seems to provide more robust and consistent models, compared to using Classical features. Analyzing lists of important features one can draw the following conclusion: the WA features of the segment 1 and 2 seems to have the highest classification "power". Interestingly, the joined features set has no WA features of segments 3 and 4.

6. Discussion and Conclusions

The results of the study show that the proposed algorithm implements the classification of adult electroretinogram signals by 19% more accurately and pediatric signals by 20% more accurately than the classical algorithm. The promising use of ERG is differential diagnostics, which may also be used in preclinical toxicology and experimental modeling. The problem of developing methods for electrophysiological signals analysis in ophthalmology

is associated with the complex morphological structure of electrophysiological signals components, due to the generation of retina cell electrical responses to light stimulus.

Author Contributions: For research articles with several authors, a short paragraph specifying their individual contributions must be provided. The following statements should be used "Conceptualization, A.E. and D.Z.; methodology, A.E., A.D. and D.Z.; software, A.E. and A.D. and A.E.; validation, V.B., A.E. and D.Z.; formal analysis, M.V.; investigation, A.D.; writing—original draft preparation, A.E.; writing—review and editing, D.Z. and M.V.; visualization, A.E.; supervision, D.Z.; project administration, A.E.; funding acquisition, M.V. All authors have read and agreed to the published version of the manuscript

Funding: The research funding from the Ministry of Science and Higher Education of the Russian Federation (Ural Federal University Program of Development within the Priority-2030 Program) is gratefully acknowledged.

Institutional Review Board Statement: Not applicable

Informed Consent Statement: Informed consent was obtained from all subjects involved in the study

Data Availability Statement: Aleksei Zhdanov, Anton Dolganov, Vasilii Borisov, Evdochim Lucian, Mikhail Ronkin, Sergey Ivliev, Vyacheslav Ponomarev, September 16, 2022, "OculusGraphy: Ophthalmic Electrophysiological Signals Database", IEEE Dataport, doi: https://dx.doi.org/10.21227/r1wb-pg25

Acknowledgments: The research funding from the Ministry of Science and Higher Education of the Russian Federation (Ural Federal University Program of Development within the Priority-2030 Program) is gratefully acknowledged.

Aleksei E. Zhdanov executed design, definition of intellectual content, data analysis, manuscript preparation and editing within the Bi-nationally Supervised Doctoral Degrees/Cotutelle DAAD Research Grant.

Conflicts of Interest: The authors declare that they have no known competing financial interests or personal relationships that could have appeared to influence the work reported in this paper.

References

1. Das, H.; Naik, B.; Behera, H.; Jaiswal, S.; Mahato, P.; Rout, M. Biomedical data analysis using neuro-fuzzy model with post-feature reduction. *Journal of King Saud University-Computer and Information Sciences* **2020**.
2. Henstridge, C.M.; Hyman, B.T.; Spires-Jones, T.L. Beyond the neuron–cellular interactions early in Alzheimer disease pathogenesis. *Nature Reviews Neuroscience* **2019**, *20*, 94–108.
3. Jamison, J.; Bush, R.; Lei, B.; Sieving, P. Characterization of the rod photoresponse isolated from the dark-adapted primate ERG. *Visual neuroscience* **2001**, *18*, 445–455.
4. Adrian, E. The electric response of the human eye. *The Journal of physiology* **1945**, *104*, 84.
5. Granit, R. Two types of retinae and their electrical responses to intermittent stimuli in light and dark adaptation. *The Journal of Physiology* **1935**, *85*, 421.
6. Creel, D.J. The electroretinogram and electro-oculogram: clinical applications by Donnell J. Creel. *Webvision: The organization of the retina and visual system* **2015**.
7. Hamilton, R.; Graham, K. Effect of shorter dark adaptation on ISCEV standard DA 0.01 and DA 3 skin ERGs in healthy adults. *Documenta Ophthalmologica* **2016**, *133*, 11–19.
8. Tang, J.; Hui, F.; Coote, M.; Crowston, J.G.; Hadoux, X. Baseline detrending for the photopic negative response. *Translational vision science & technology* **2018**, *7*, 9–9.
9. Bach, M.; Meroni, C.; Heinrich, S.P. ERG shrinks by 10% when reducing dark adaptation time to 10 min, but only for weak flashes. *Documenta Ophthalmologica* **2020**, *141*, 57–64.
10. McCulloch, D.L.; Marmor, M.F.; Brigell, M.G.; Hamilton, R.; Holder, G.E.; Tzekov, R.; Bach, M. ISCEV Standard for full-field clinical electroretinography (2015 update). *Documenta ophthalmologica* **2015**, *130*, 1–12.
11. Lyons, J.S.; Severns, M.L. Using multifocal ERG ring ratios to detect and follow Plaquenil retinal toxicity: a review. *Documenta ophthalmologica* **2009**, *118*, 29–36.
12. Robson, A.G.; Webster, A.R.; Michaelides, M.; Downes, S.M.; Cowing, J.A.; Hunt, D.M.; Moore, A.T.; Holder, G.E. "Cone dystrophy with supernormal rod electroretinogram": a comprehensive genotype/phenotype study including fundus autofluorescence and extensive electrophysiology. *Retina* **2010**, *30*, 51–62.

13. Johnson, M.A.; Jeffrey, B.G.; Messias, A.; Robson, A.G. ISCEV extended protocol for the stimulus–response series for the dark-adapted full-field ERG b-wave. *Documenta Ophthalmologica* **2019**, *138*, 217–227.
14. Moskowitz, A.; Hansen, R.M.; Fulton, A.B. ERG oscillatory potentials in infants. *Documenta ophthalmologica* **2005**, *110*, 265–270.
15. Li, X.X.; Yuan, N. Measurement of the oscillatory potentials of the electroretinogram in the domains of frequency and time. *Documenta ophthalmologica* **1990**, *76*, 65–71.
16. Wan, W.; Chen, Z.; Lei, B. Increase in electroretinogram rod-driven peak frequency of oscillatory potentials and dark-adapted responses in a cohort of myopia patients. *Documenta Ophthalmologica* **2020**, *140*, 189–199.
17. Nair, S.S.; Joseph, K.P. Wavelet based electroretinographic signal analysis for diagnosis. *Biomedical Signal Processing and Control* **2014**, *9*, 37–44.
18. Zhdanov, A.E.; Borisov, V.I.; Dolganov, A.Y.; Lucian, E.; Bao, X.; Kazaijkin, V.N. OculusGraphy: Norms for electroretinogram signals. In Proceedings of the 2021 IEEE 22nd International Conference of Young Professionals in Electron Devices and Materials (EDM). IEEE, 2021, pp. 399–402.